Altered Subcellular Localization and Low Frequency of Mutations of ING1 in Human Brain Tumors

Diego Vieyra,[1] Donna L. Senger,[1] Tatsuya Toyam,[2] Huong Muzik,[1] Penny M. A. Brasher,[3] Randal N. Johnston,[1,4] Karl Riabowol,[1] and Peter A. Forsyth[5]

[1]Departments of Medical Biochemistry and Oncology and Southern Alberta Cancer Research Center, The University of Calgary, Calgary, Alberta, Canada; [2]Department of Surgery II, Nagoya City University Medical School, Nagoya, Japan; [3]Division of Epidemiology, Prevention and Screening, Tom Baker Cancer Center, Calgary, Alberta, Canada; [4]Genome Prairie, Calgary, Alberta, Canada; and [5]Department of Oncology and Clinical Neuroscience, The University of Calgary and Tom Baker Cancer Center, Calgary, Alberta, Canada

ABSTRACT

Purpose: **Clinical and experimental evidence suggest that the p33^{ING1b} candidate tumor suppressor functionally cooperates with p53 in controlling biochemical and biological functions. Because p53 is frequently mutated in brain tumors and the ING1 locus maps to a site of which the loss is associated with gliomas, we analyzed the mutation and expression profiles of ING1B in human brain tumors. Here we present the first report of ING1 expression and mutation analyses in human brain tumor samples and malignant glioma cell lines.**

Experimental Design: **Expression and mutation analyses of ING1B together with subcellular localization studies of ING1 proteins were performed on 29 brain tumor specimens and 6 human glioma cell lines.**

Results: **A single point mutation (3.5%) was detected in the 29 brain tumor specimens analyzed. This missense mutation occurred in a sequence reported previously to confer nuclear translocation properties to p33^{ING1b}. Interestingly, overexpression and subcellular mislocalization of p33^{ING1b} were observed in all 29 of the brain tumor specimens and some glioma cell lines. In tumor samples, ING1 proteins aberrantly localized to the cytoplasm, and to a lesser extent, to the nucleus of glioma cells.**

Conclusions: **Our data indicate that although mutations of ING1 seem to be infrequent in human brain tumors, deregulated expression and mislocalization of ING1 proteins, particularly the p33^{ING1b} isoform, are common events in gliomas and glioblastomas.**

INTRODUCTION

The p33^{ING1b} protein, encoded by ING1B (1) and known previously as p33^{ING1} (2), is the best-characterized and most widely expressed isoform of the ING1 candidate tumor suppressor. Suppression of ING1B expression promotes focus formation and cell growth *in vitro* and tumor formation *in vivo* (2). Ectopic overexpression of p33^{ING1b} blocks cell cycle progression (2–4), and sensitizes cells to apoptosis in diverse human and murine models (4–12). In human glioma cell lines, adenovirus-mediated expression of ING1B highly sensitizes cells to p53-dependent apoptosis (6). In addition, p33^{ING1b} is able to up-regulate the expression of proapoptotic and cell cycle regulatory p53-dependent proteins like Bax (11, 12) and the cyclin-dependent kinase inhibitor p21^{WAF1} (3, 10, 12, 13), respectively. These properties seem to be subject to controlled subcellular localization of p33^{ING1b} (7, 8) and involve physical associations of this protein with other nuclear-targeted proteins such as p53 (3, 12, 14), proliferating cell nuclear antigen (8, 10), DNA repair proteins (15), specific histone acetyltransferases (10), and histone deacetylases (10, 16), as well as chromatin (4). These data suggest that ING1 proteins, and particularly p33^{ING1b}, could provide a direct linkage among DNA repair, apoptosis, cell cycle, and chromatin remodeling via multiple protein complexes that are assembled in the nucleus (Refs. 4, 10; reviewed in Ref. 17). Indeed, experimentally introduced mutations in either the proliferating cell nuclear antigen-interacting sequence (8) or the nuclear localization domain of p33^{ING1b} (7) impair its proapoptotic effect in normal human cells.

The locus of ING1 maps to chromosome 13q33–34 (18), a site associated frequently with loss of heterozygosity in several types of cancers (19–24), including glioblastomas (25–27). Clinical studies have shown that mutations and/or down-regulation of p33^{ING1b} has been linked to cancer of the breast (28), liver (29), stomach (30), and squamous cell carcinomas (31–33), as well as lymphoid (34, 35), thyroid (35), testicular (35), melanocytic (35, 36), and hematological (37) malignancies, consistent with ING1 acting as a class 2 tumor suppressor (38). Whereas down-regulation of ING1B is the most frequent alteration of ING1 associated with cancer (28–37), up-regulation (39) and subcellular mislocalization (35–37) of p33^{ING1b} have also been linked to human malignancies. For example, decreased nuclear localization and/or increased cytoplasmic localization of p33^{ING1b} have been associated with melanoma (35,

Received 4/7/03; revised 8/11/03; accepted 8/14/03.
Grant support: Alberta Cancer Board (ACB), the Canadian Cancer Society of the National Cancer Institute of Canada (NCIC), and the Canadian Institutes of Health Research (CIHR; P. F. and K. R.). K. R. is a CIHR and Alberta Heritage Foundation for Medical Research (AHFMR) Scientist. D. V. receives doctoral studentships from the CIHR, AHFMR, and ACB. D. S. receives a postdoctoral fellowship from the AHFMR.
The costs of publication of this article were defrayed in part by the payment of page charges. This article must therefore be hereby marked *advertisement* in accordance with 18 U.S.C. Section 1734 solely to indicate this fact.
Note: D. V. and D. L. S. contributed equally to the work.
Requests for reprints: Peter A. Forsyth, Depts. Clinical Neurosciences, Oncology and Pediatrics, Tom Baker Cancer Center, 1331 29 Street N.W., Calgary, Alberta, Canada T2N 4N2. Phone: (403) 670-2000; Fax: (403) 283-1651; E-mail: peterfo@cancerboard.ab.ca.

36), seminoma (35), papillary thyroid carcinoma (35), ductal breast carcinoma (35), and acute lymphoblastic leukemia (35, 37). Furthermore, loss of nuclear expression and increased cytoplasmic staining of $p33^{ING1b}$ have been observed in 78% of patients with acute lymphoblastic leukemia (37). Finally, a low frequency of mutations and overexpression of $p33^{ING1b}$ have been reported recently in highly malignant human melanocytic cell lines (39). All of these studies support the idea that misregulation of ING1 proteins may contribute to pathways important in cell transduction (17).

Experimental evidence indicates that $p33^{ING1b}$ functionally cooperates with p53 in controlling cell growth (3, 10, 12, 14, 40), apoptosis (4, 6, 9, 10, 15) and senescence (4, 41). Because p53 is frequently mutated in brain tumors (42–45) and the ING1 locus maps to a site of which the loss is associated with gliomas (25–27), functional loss of ING1 might contribute to tumorigenesis of human brain tumors. To test this hypothesis we examined the mutational status of ING1, the expression profile of ING1B, and the subcellular localization of $p33^{ING1b}$ in glioma cell lines and primary human brain tumors. Here we present the first report of $p33^{ING1b}$ expression and mutation analyses in brain tumor samples and human MG[6] cell lines.

MATERIALS AND METHODS

Tumor Tissues and Cell Lines. Tumor and normal tissues were obtained from the Canadian Brain Tumor Tissue Bank in London, Ontario, and the Calgary Foothills Hospital. Briefly, tissue was taken during surgery while patients were under a general anesthetic, and was placed immediately in liquid nitrogen and stored at −80°C. An institutional ethics board approved the collection and use of all of the surgical tissue used, and all of the patients gave signed informed consent. The following tissues were studied: 18 GBMs, 4 AAs, 4 LGs, and 18 Ms including 6 MMs. These were compared with 7 controls obtained during nonbrain tumor surgery. From these 44 samples all were suitable for RNA, and 29 gave suitable yields of DNA and protein. Six MG cell lines were obtained from different sources including the American Tissue Culture Collection (U87, A172, and SNB19), Penny Costello (University of Western Ontario, London, Ontario, Canada) (U343), Voon Wee Yong (University of Calgary, Calgary, Alberta, Canada) (U251), and Charles Wilson (University of California at San Francisco, San Francisco, CA) (SF188). These were compared with cultured human fetal astrocytes (obtained from Voon Wee Yong). All of the cells were grown in DMEM-F12 containing 10% FCS; cells were passaged when they reached ~80% confluence and harvested for DNA, RNA, or protein by standard procedures (46, 47).

DNA, RNA, and Protein Extraction. For DNA extraction, samples were homogenized in Saline Tris EDTA buffer [100 mM Tris-HCl (pH 8.0), 10 mM NaCl, and 1 mM EDTA (pH 8.0)] with 50 μg/ml proteinase K and 0.1% SDS, and incubated at 50°C for 3–4 h. Genomic DNA was extracted using the phenol-chloroform method (46). Total RNA was extracted from cells by the acid guanidinium isothiocyanate method (47). The final RNA concentrations were determined by adsorption using a geneQuant spectrophotometer (Pharmacia). Protein was prepared by boiling samples in 2× Laemmli sample-buffer before electrophoresis.

RT-PCR. *ING1* mRNA expression in tumor and normal tissues was monitored by duplex RT-PCR (48). Each 20-μl cDNA synthesis reaction contained 1 μl of total RNA from tumor or normal cells, buffer [10 mM Tris-HCl (pH 9.0), 50 mM KCl, and 1.5 mM $MgCl_2$], 1 mM each of deoxynucleoside triphosphates, 25 units of RNAguard RNase inhibitor (Pharmacia Biotech Inc., Baie dU'rfé, Quebec, Canada), 200 units of Superscript II reverse transcriptase (Life Technologies, Inc.), and 100 ng of $pd(N)_6$ random hexamer (Pharmacia). One-μl of each room temperature reaction was amplified using 1 unit of TaqDNA polymerase (Pharmacia). Thirty-three PCR cycles for *ING1*B (forward primer: 5′-CTC CAT CGA GTC CCT GCC TT-3′; reverse primer: 5′-GCC TTC TTC TCC TTG GGT GT-3′) and 22 PCR cycles for *GAPDH* (forward primer: 5′-CGG AGT CAA CGG ATT TGG TCG TAT-3′, reverse primer: 5′-AGC CTT CTC CAT GGT GGT GAA GAC-3′) were used for amplification consisting of 1 min at 94°C, 1 min at 62°C, and 1 min at 72°C, with a 5 min extension at 72°C after the last cycle. Primers for *GAPDH* were added to PCR tubes at the end of the 11th cycle. PCR reactions were run three times to confirm reproducibility.

PCR-SSCP Analysis. PCR reactions were carried out in a volume of 50 μl containing 200 ng of genomic DNA, 1.5 mM $MgCl_2$, 50 mM KCl, 10 mM Tris-HCl (pH 9.0), 0.2 mM of each deoxynucleoside triphosphates, 0.5 μM of each primer, and 1 unit TaqDNA polymerase (Pharmacia). Thirty cycles were used for amplification consisting of 1 min at 94°C, 1 min at 60°C, and 1 min at 72°C, with a 5-min extension at 72°C after the last cycle. PCR-SSCP analysis was performed by a nonradioisotopic method (28). An 8-μl aliquot of PCR product was added to 8 μl of loading buffer (0.05% bromphenol blue and 0.05% xylene cyanol in deionized formamide; Sigma, Oakville, Ontario, Canada). The mixture was heat-denatured at 95°C for 10 min and snap-chilled on ice. The single-stranded PCR product was then loaded onto 8–10% polyacrylamide-TBE [44.5 mM Tris-borate and 1 mM EDTA (pH8.0)] gels with or without 10% glycerol at 4°C. Gels were electrophoresed for 1.5–4 h at 600 V and were stained with ethidium bromide (1.0 μg/ml) for 10 min. The bands were visualized on a transilluminator. Gels were photographed using Polaroid film. The sequences of the *ING1* primers for PCR-SSCP analysis were as follows; primer-I [forward primer: 5′-CTG AAG GAG CTA GAC GAG TG-3′ (nucleotides 201–221), reverse primer: 5′-GGC TTG TCA GAC TGC GCT AC-3′ (nucleotides 474–494)], primer-II [forward primer: 5′-GTA GCG CAG TCT GAC AAG CC-3′ (nucleotides 474–494), reverse primer: 5′-ACG CAC GAG AAG TGG AAC CA-3′ (nucleotides 763–783)], and primer-III [forward primer: 5′-GAC AAC GAC GAG TGC CCC AT-3′ (nucleotides 739–759), reverse primer: 5′-CTA CCT GTT GTA AGC CCT CTC

[6] The abbreviations used are: MG, malignant glioma; GBM, glioblastoma multiforme; AA, anaplastic astrocytoma; LG, low-grade glioma; M, meningioma; MM, malignant meningioma; RT-PCR, reverse transcription-PCR; GAPDH, glyceraldehyde-3-phosphate dehydrogenase; SSCP, single-strand conformational polymorphism; DAB, 3,3′-diaminobenzidine.

T-3′ (nucleotides 879–901)]. Reproducibility was confirmed by PCR-SSCP methods in all of the abnormal samples.

Direct Sequencing of PCR Products. Abnormal bands detected by PCR-SSCP analysis were excised and reamplified by PCR. This PCR product was purified using a Geneclean II kit (BIO 101 Inc., Vista, CA). Sequencing was performed by using a model 373A version 1.2.0 genetic analyzer by the Southern Alberta DNA Synthesis and Sequence Facility.

***In Situ* Hybridization.** A 987bp *Eco*RI-*Xho*I fragment of *ING1* was cloned into a pBK-CMV phagemid (Stratagene Cloning System, La Jolla, CA). Antisense riboprobe was generated with T3 RNA polymerase from template linearized with *Eco*RI, and sense riboprobe was produced with T7 RNA polymerase and *Xho*I-digested plasmid. *In situ* hybridization was performed as described previously (28). Briefly, 8-μm paraffin-embedded tissue sections were dewaxed in xylene and rehydrated through a series of graded ethanol solutions. Sections were treated with proteinase K (20 μg/ml), acetylated, and then prehybridized in buffer containing 50% formamide, 5× saline-sodium phosphate-EDTA (3 M NaCl, 173 mM NaH_2PO_4, and 25 mM EDTA), and 1× Denhardt's solution (0.02% BSA, 0.02% Ficoll 400, and 0.02% polyvinylpyrrolidone) for 6 h at 60°C. Hybridization was done at 60°C overnight in the same buffer to which 10 ng/ml of probe and 8 μg/ml of *Escheria coli* tRNA were added. After hybridization, sections were washed once in 2× SSC at 37°C, treated with 40 μg/ml RNase A at 37°C, and washed sequentially in 2× SSC at 37°C, 2× SSC at room temperature, 1× SSC at room temperature, 0.5× SSC at room temperature, and in 0.1× SSC at 50°C. After blocking, sections were incubated in mouse monoclonal antibody against digoxigenin (Boehringer Mannheim) overnight at 4°C. Goat anti-mouse horseradish peroxidase (Pierce) was used as secondary antibody. Visualization of peroxidase was made by using DAB (Sigma) substrate, enhanced in 0.5% copper sulfate, and hematoxylin was used as a nuclear counterstain. Sections were photographed with Kodak Royal Gold 35-mm film using an Olympus BH-2 photomicroscope under bright field illumination.

Immunohistochemistry. For immunolocalization of $p33^{ING1b}$, an indirect immunoperoxidase method was used. In brief, formalin-fixed, paraffin-embedded tissue sections were reacted with a mixture of four mouse anti-ING1 monoclonal antibodies (49) for 16 h at 4°C followed by biotinylated horse antimouse/antirabbit (Vector). Avidin-biotin peroxidase complexes were formed using an "ABC" kit (Vector). DAB was converted to brown reaction product by peroxidase, and hematoxylin was used as a blue nuclear counterstain.

Indirect Immunofluorescence. Human MG cell lines were grown on glass coverslips for 48 h at 37°C to 60% confluence as described previously (50). The cells were then fixed in 3.7% formaldehyde, washed in 0.5% Triton X-100 and 0.05% Tween 20 for 10 min each at room temperature. Formaldehyde and detergents were diluted in PBS [137 mM NaCl, 8.1 mM Na_2HPO_4, 2.68 mM KCl, and 1.47 mM KH_2PO_4 (pH 7.5)]. The cells were incubated for 30 min with a mixture of four monoclonal antibodies against ING1, washed in PBS with 0.05% Tween 20. After washing, cells were incubated with the secondary antibody goat antimouse IgG (Alexa 488; Cedarlane). After rinsing, the samples were mounted in 1 μg/ml paraphenylenediamine in PBS/90% glycerol that also contained the DNA-specific dye 4′,6-diamidino-2-phenylindole at 1 μg/ml. Imaging was performed using a 14-bit cooled CCD camera (Princeton Instruments) mounted on a Leica DMRE immunofluorescence microscope.

Western Blotting. Protein extracts were prepared as follows. Samples of ~3 mm^3 were taken from human glioma biopsies and stored at −80 C°. The samples were washed with ice-cold PBS and were immersed in ice-cold extraction buffer after which they were homogenized and sonicated on ice. These samples were centrifuged 10 min at 13,000 rpm at 4 C°, and their supernatants were recovered and stored at −20 C° for Western blot assays. Human MG cells growing in 100-mm tissue culture dishes (~3×10^6 cells/dish) were washed with ice-cold PBS and dissolved in the above extraction buffer following the same procedure as that for the tissue samples.

Protein samples were quantitated by Bradford assay, and solubilized in 2× Laemmli sample buffer, run on 15% SDS-PAGE gels, and transferred to PolyScreen microporus polyvinylidene difluoride membranes (NEN Life Science Products, Boston, MA). Membranes were blotted using a 1:2 dilution of ING1 monoclonal antibodies [Cab1, Cab2, Cab3, and Cab4 (49) in equal proportions] and detected by chemiluminescence using the Amersham enhanced chemiluminescence kit according to the manufacturer's instructions.

Statistical Analysis. Levels of mRNA expression as estimated using RT-PCR and scanning densitometry were compared using Student's *t* test. The levels of expression in various grades of gliomas and 7 normal brain specimens were compared using the Kruskal-Wallis test. Protein levels on Western blots were described qualitatively.

RESULTS

Low Frequency of Mutation of the ING1 Gene in Primary Brain Tumors. Because mutations in ING1 have been found in a variety of cancers (2, 28, 30–33), we screened 29 brain tumor specimens for ING1 mutations using PCR-SSCP analysis. DNA sequences were determined for any PCR product that showed a variant pattern by SSCP. The following tissues were studied: 5 GBMs, 4 AAs, 4 LGs, and 12 Ms including 4 MMs. These were compared with 4 control tissues obtained during nonbrain tumor surgery. A single missense mutation was detected. The tumor DNA from case BT-38 (meningioma) had a G-to-A transition at position 239 of the ING1B coding sequence (Fig. 1*A*; Pubmed accession no. for ING1B: AAF07921). This mutation resulted in an arginine to histidine substitution in codon 80 of ING1B cDNA (Fig. 1*C*). This alteration, however, was not present in the corresponding normal lymphocyte DNA from this patient (Fig. 1*B*) indicating that this was a somatic mutation. Furthermore, the expression of ING1B was not reduced in this tumor sample. Interestingly, this mutation occurred in a sequence reported previously to confer nuclear translocation properties to $p33^{ING1b}$. For instance, a fusion protein containing green fluorescence protein attached to the amino acid sequence 1–150 of $p33^{ING1b}$ localized to the nucleus when microinjected in normal human cells (7).

Higher Levels of ING1B mRNA in MG Cell Lines Compared with Primary Human Astrocytes. Because transcriptional dysregulation of ING1B has been observed in di-

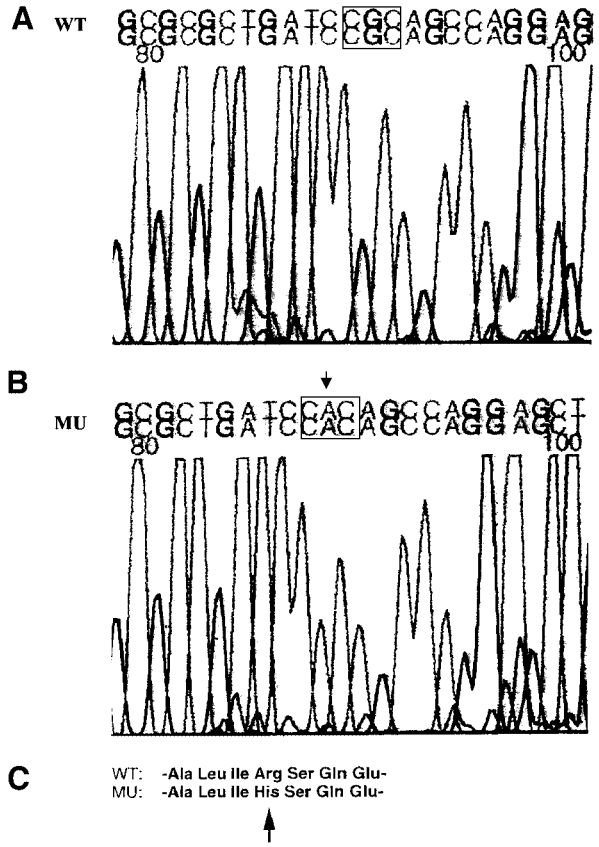

Fig. 1 Presence of a somatic mutation of ING1 in human brain tumors. *A,* ING1B wild-type sequence. The *square* indicates the position of codon 80 of ING1B. This codon encodes arginine. *B,* somatic mutation found in brain tumor sample (a meningioma). The *arrow* indicates the G-to-A transition that leads to histidine in codon 80 of ING1B. *C,* translated codons for the sequences shown in *A* and *B,* indicating that the mutation is translated to histidine instead of arginine. *WT,* wild-type ING1B sequence; *MU,* mutant ING1B sequence.

verse types of tumors and cancer cell lines (28–37, 39), we analyzed the mRNA expression profiles of ING1B in both glioma cell lines and primary human brain tumors. We used the RT-PCR primer-dropping method that includes internal RNA loading controls (GAPDH) in every sample (48). To eliminate the potential contribution of genomic DNA to our analysis, PCR primers were designed to span an intron sequence (28). The level of ING1B mRNA from six MG cell lines was compared with cultured human astrocytes. As shown in Fig. 2*A*, ING1B mRNA levels were highly variable among the glioma cell lines. Two cell lines (U251 and U343) displayed levels of ING1B mRNA similar to normal human fetal astrocytes, whereas four of the cell lines (SF188, A172, SNB19, and U87) displayed higher levels of ING1B mRNA. On average, ING1B levels were elevated in glioma lines compared with normal astrocytes (one sample *t* test, $P = 0.0033$). Fig. 2*A* shows average values referred to the fetal astrocyte sample average value. To determine whether the ING1B expression profiles observed in glioma cell lines correlated with those from human brain tumors, we then characterized the RNA expression profile of ING1B in brain tumor samples.

High and Variable Levels of ING1B mRNA in Primary Human Brain Tumors. The expression level of ING1B mRNA examined in 29 primary brain tumors was compared with those of 7 normal human brain tissues obtained from brain surgery of areas unrelated to cancer. As shown in Fig. 2*B*, the expression levels of ING1B were significantly higher in the different types of tumor specimens than in the normal brain tissues. Average expression levels of ING1B were 0.67, 1.92, 1.67, 1.18, 1.21, and 1.36 (arbitrary units) for samples of normal brain, LGs, MGs, GBMs, M, and MM, respectively. These differences were shown to be statistically significant (Kruskal-Wallis test, $P = 0.0073$). Fig. 2*B* shows that values referred to the average value of the normal samples.

p33^{ING1b} Expression Parallels ING1B mRNA Levels. We have shown previously that levels of ING1B mRNA frequently parallel p33^{ING1b} levels in both human diploid fibroblasts (2, 4, 41) and many cancer cell lines (2, 28), suggesting that p33^{ING1b} is regulated primarily at the transcriptional level (2, 4). To answer whether p33^{ING1b} expression similarly correlated with its mRNA expression in glio-

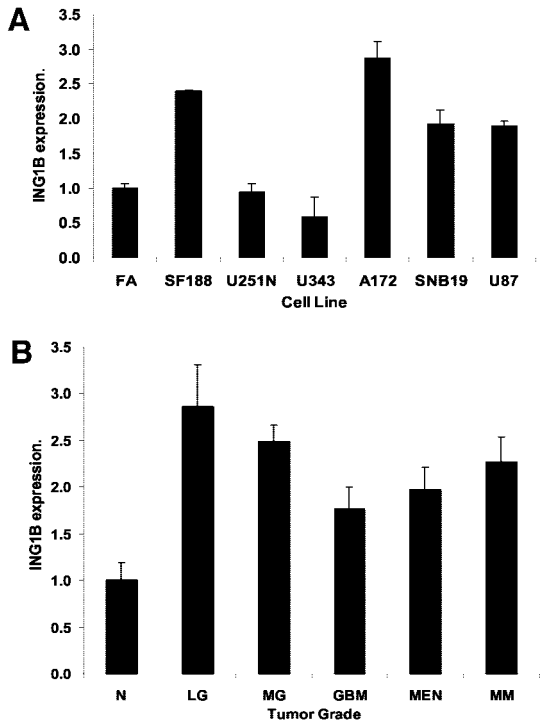

Fig. 2 High expression of ING1B mRNA in MG cell lines and human brain tumor specimens. Deregulated expression of ING1B mRNA. *A,* RT-PCR analysis on malignant human glioma cell lines. In 4 of 6 cell lines, ING1B mRNA expression was up-regulated compared with normal fetal astrocytes (*FA*; *t* test, $P = 0.0033$). Average values are referred to the average value of the fetal astrocyte sample. *B,* RT-PCR analysis of brain tumor surgical specimens. ING1B mRNA expression level in tumor specimens were significantly higher than in normal brain tissues (Kruskal-Wallis test, $P = 0.0073$). Averages values are referred to the average value of the normal sample. *n,* normal human brain tissue ($n = 7$); LG ($n = 4$); MG ($n = 4$); GBM ($n = 18$); *MEN,* meningioma ($n = 11$); MM ($n = 5$).

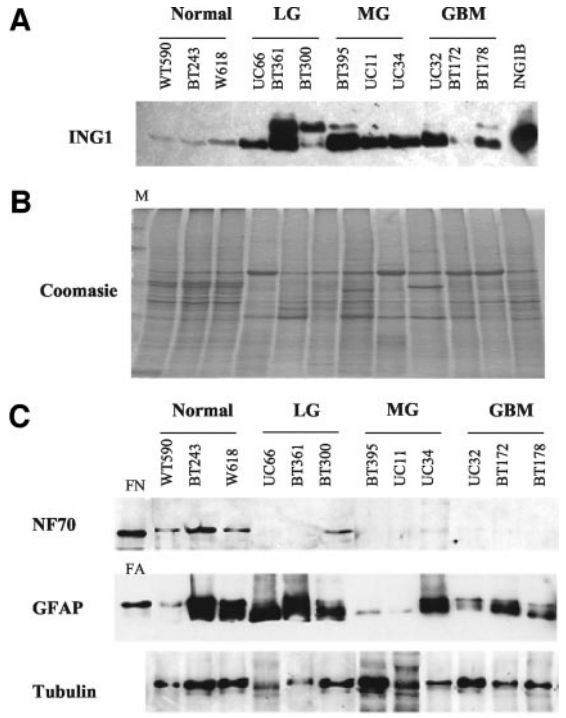

Fig. 3 Deregulated expression of $p33^{ING1b}$ in primary brain tumor specimens. *A,* Western immunoblot analysis of $p33^{ING1b}$ on randomly chosen samples of normal and tumor specimens from Fig. 2*B*. *Normal,* normal brain; *ING1B,* protein extract of normal human fibroblast transfected with INGIB expression construct. Note that $p33^{ING1b}$ levels correlate with levels of ING1B mRNA (Fig. 2*B*). *B,* Coomassie Brilliant Blue stained gel of samples run in *A* as a parallel loading control. Lanes are ordered the same as in *A*. *M,* molecular weight protein marker. *C,* Western immunoblot analysis of neuronal (*NF-70*) and glial (*GFAP*) markers in samples shown in *A*. *Normal,* normal brain; *FN,* fetal neurons (*neuron control*); *FA,* fetal astrocytes (*glia control*).

mas, we examined the relationship between ING1B mRNA and $p33^{ING1b}$ levels in normal brain tissue ($n = 3$), and tumor specimens ($n = 9$); the latter including LGs, MGs, and GBM. These experiments were performed with a mixture of previously characterized mouse monoclonal antibodies raised against the COOH-terminal end of $p33^{ING1b}$ (49). As shown in Fig. 3*A*, the relative levels of $p33^{ING1b}$ were similar to those observed by the RT-PCR approach for ING1B mRNA (compare Fig. 2*B* with Fig. 3*A*). However, the magnitude of differences seen between protein levels in normal *versus* cancer tissues was much greater than that seen for mRNA. This was particularly evident in some samples such as BT361, BT300, BT395, and BT178, all of which also showed the presence of an additional higher molecular weight reactive polypeptide. This additional protein may be a result of rearrangements of one allele, alternative splicing of the $p47^{ING1a}$ variant or post-translational modifications of $p33^{ING1b}$. Our preliminary result does not support the idea that it represents $p47^{ING1a}$, and so it may represent a tumor-specific alteration of the ING1 gene products. Fig. 3*B* shows that similar amounts of protein were analyzed, and Fig. 3*C* gives the relative contribution of glial and neuronal compartments in each surgical specimen shown in Fig. 3*A*, because GFAP and NF70 are glia-specific and neuron-specific markers, respectively. These controls suggest that the glia compartment contributes to the majority of the signal seen for $p33^{ING1b}$.

Cell-Dependent Expression of ING1B mRNA in Both Normal and Brain Tumor Specimens. To determine the identity of the cell types expressing $p33^{ING1b}$, we studied the expression of ING1B by an RNA *in situ* hybridization approach and compared these data with immunohistochemistry data on $p33^{ING1b}$. For both analyses, we used normal brain biopsies and a number of brain tumor samples spanning the spectrum of glioma malignancies as indicated previously. Fig. 4 shows results from the RNA *in situ* hybridization approach. As shown in the left panel, ING1B mRNA was expressed in neurons and blood vessels in normal brain. Conversely, tumor samples displayed positive ING1B mRNA staining in tumor cells and in blood vessels in gliomas of all grades (second to fourth panels). ING1B expression was visualized by DAB (brown), whereas hematoxylin was used as a nuclear counterstain (dark blue).

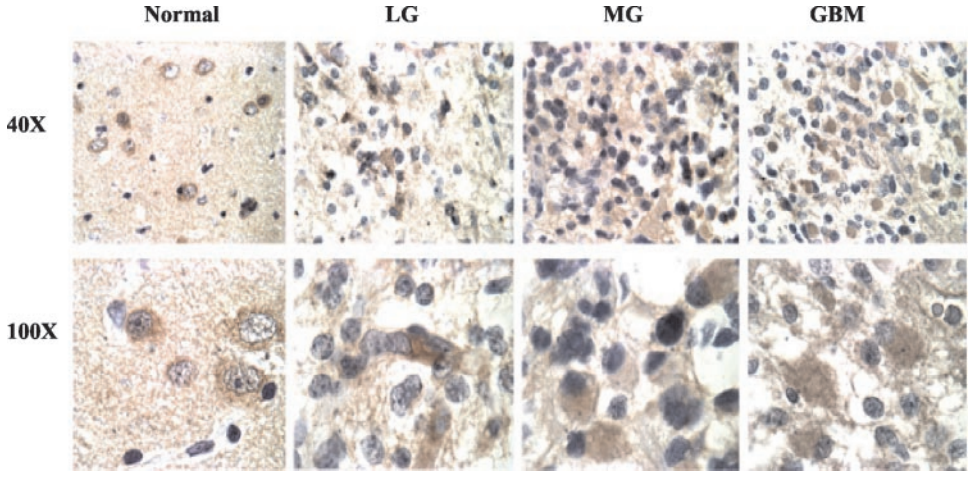

Fig. 4 Cell-specific expression of ING1B mRNA in normal and primary brain tumor samples. RNA *in situ* hybridization analysis of ING1B in normal human brain and tumor tissues. *A,* DIG-labeled antisense ING1 mRNA probe was incubated with tissue preparations of surgical specimens spanning the spectrum of glioma malignancies. *Normal,* normal brain. Microscopy magnifications (×40 and ×100) are indicated on the *left*. Hybridization with a sense ING1 gene probe as a negative control showed no signal (data not shown).

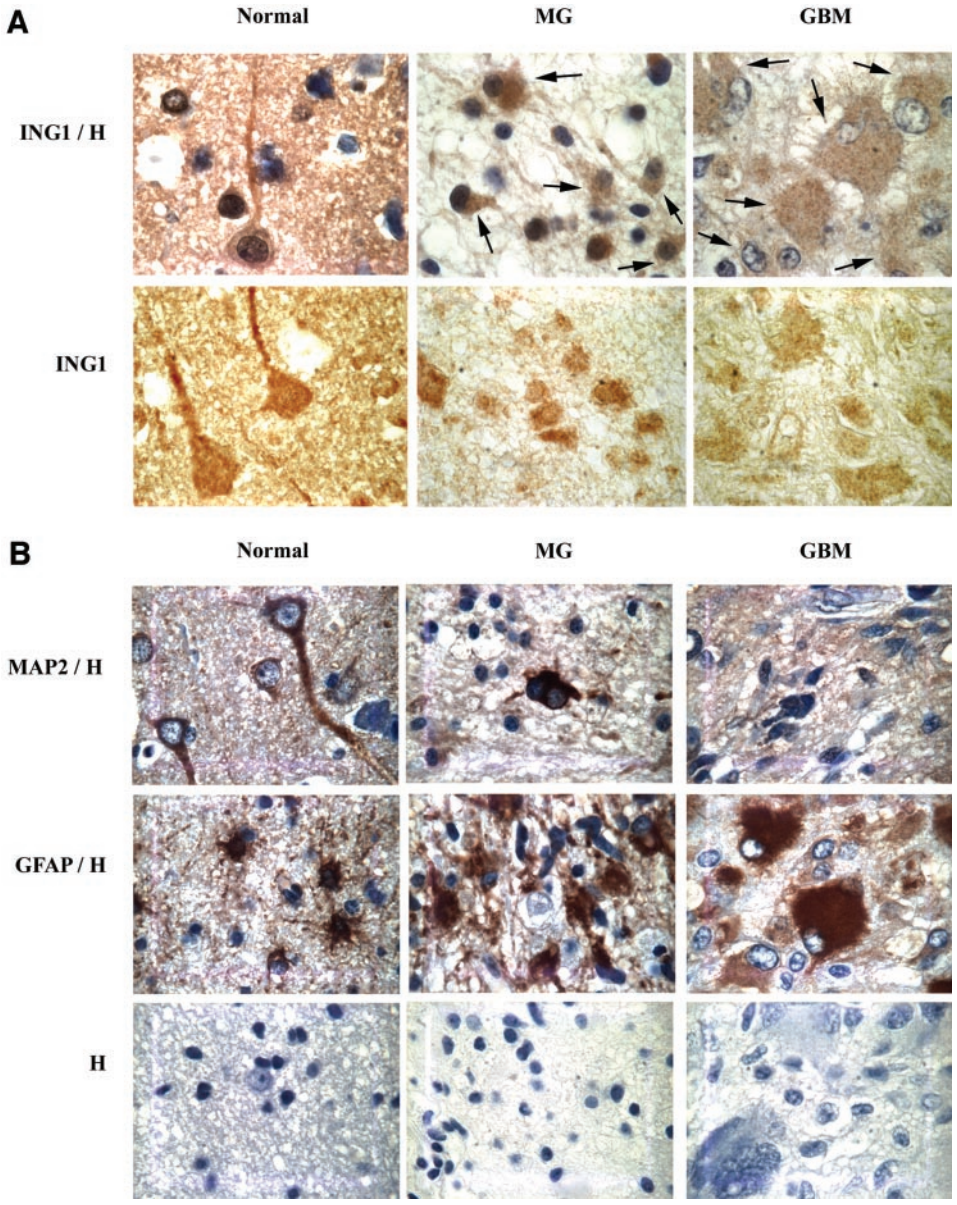

Fig. 5 Cytoplasmic localization of p33^{ING1b} in glioma surgical specimens. *A*, p33^{ING1b} staining in normal and tumor brain tissue. *H*, hematoxylin; *Normal*, normal brain. Magnification: ×100. *Arrows* shows some examples of tumor cells where p33^{ING1b} staining is cytoplasmic. *B*, characterization of normal and tumor tissue for glial (*GFAP*) and neuronal (*MAP2*) markers. *Normal*, normal brain; *H*, hematoxylin. Magnification: ×100.

Cytoplasmic Localization of p33^{ING1b} in Human MG Surgical Specimens and Glioma Cell Lines. Previous studies have demonstrated that p33^{ING1b} localizes to the nucleus of cells in normal human and murine diploid fibroblast cell cultures (2, 5, 7, 41), as well as in normal human tissues (35). Several studies have reported recently that both loss of nuclear localization and increased cytoplasmic localization of p33^{ING1b} was associated with specific types of tumors (35–37). Because our mutation analysis of brain tumor samples indicated the presence of a mutation in a sequence demonstrated previously to confer nuclear localization properties to p33^{ING1b} (7), we studied the subcellular distribution of p33^{ING1b} in glioma specimens and human MG cell lines. Fig. 5 shows representative pictures of p33^{ING1b} staining in human glioma surgical specimens using a mixture of ING1 monoclonal antibodies (49). As shown in Fig. 5*A* (middle and right panels), p33^{ING1b} avidly localized to the cytoplasm of tumor cells in both MG and GBM specimens. This cytoplasmic localization of p33^{ING1b} was restricted to the GFAP0-positive cells (Fig. 5*B*), indicating that the mislocalization of p33^{ING1b} was associated with malignant glia. Similar to the results derived from the RNA *in situ* hybridization analysis, this immunohistochemistry study showed that the expression of p33^{ING1b} was cell-dependent. For example, we were unable to find p33^{ING1b}-positive staining of glia in normal brain tissues, although neurons displayed positive staining (Fig. 5A, left panels). Notably, in no instance did we observe exclusive nuclear p33^{ING1b} immunoreactivity in the glioma specimens. To examine the subcellular distribution of p33^{ING1b} in human MG cell lines, we performed indirect immunofluorescence on two (randomly chosen) cell lines (U251 and SNB19). As shown in Fig.

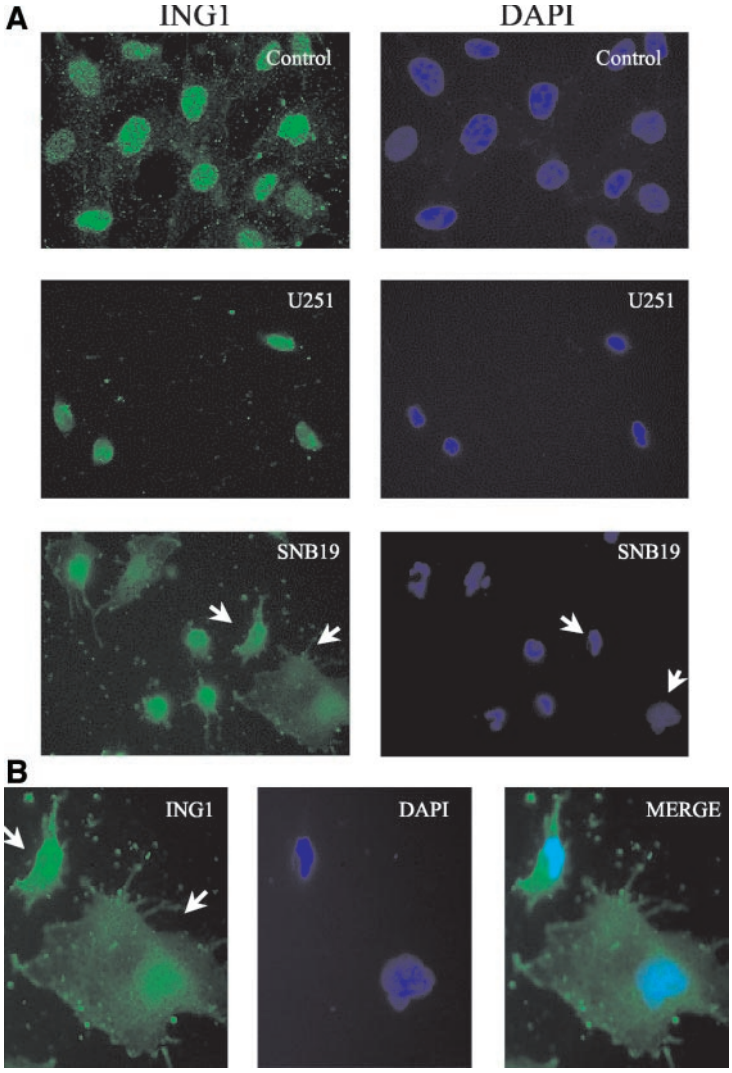

Fig. 6 Increased cytoplasmic localization of $p33^{ING1b}$ in the SNB19 glioma cell line. *A*, cell lines from Fig. 2*A* were grown on coverslips, fixed, stained for $p33^{ING1b}$ (*green*), nuclear DNA (4′,6-diamidino-2-phenylindole, in *blue*), and analyzed by indirect immunofluorescence microscopy. Note that SNB19 displays both nuclear and cytoplasmic distribution of $p33^{ING1b}$, whereas U251 and the normal control fibroblasts display nuclear staining for $p33^{ING1b}$. Magnification: ×100. *Arrows* identify cells shown in *B*. *B*, magnification, ×600. Note the intense cytoplasmic staining of $p33^{ING1b}$ (*green*) in SNB19 cells.

6*A*, although we found variable staining for $p33^{ING1b}$ between the nuclear and cytoplasmic compartments of these glioma cell lines, U251 and the normal human control (HS68 fibroblasts) showed clear nuclear localization, whereas SNB19 has both a nuclear and cytoplasmic distribution of ING1. The intense cytoplasmic staining of $p33^{ING1b}$ in SNB19 (Fig. 6*B*) corroborated results derived from immunohistochemistry of tumor specimens (Fig. 5*A*, middle and left panels).

DISCUSSION

This study makes three observations about ING1 in human brain tumors. First, the ING1 gene is mutated at a low frequency in human brain tumors. Second, the expression level of ING1B is significantly different in brain tumor specimens compared with normal brain. Third, the protein distribution of $p33^{ING1b}$ is atypical in some glioma cell lines and in all of the tumor specimens where it is, evidently, increased in the cytoplasm.

A single point mutation was detected in 29 brain tumor specimens (3.5%). This G-to-A transition resulted in an arginine to histidine substitution that did not cause altered expression of ING1B mRNA. Although the functional significance of this mutation is still unknown, the fact that it occurred within a region of ING1 reported previously to target $p33^{ING1b}$ to the nucleus (7) is highly suggestive of an aberrant regulatory role. For instance, we have shown that, although $p33^{ING1b}$ has a bipartite nucleolar targeting sequence between amino acids 142 and 194, the sequence 1–150 has strong nuclear localization properties (7). Indeed, a fusion protein containing green fluorescence protein linked to the amino acid sequence 1–150 of $p33^{ING1b}$ localized to the nucleus when microinjected in normal human cells (7). Consisting of the idea that the mutation we found might affect regulatory functions of $p33^{ING1b}$, arginine 80 is part of a consensus phosphorylation site for the ataxia-telangiectasia mutatedprotein kinase, which would phosphorylate serine 81 (results derived from Motif Scanner; Ref. 51). However, these speculations are currently being tested.

Consistent with the rarity of ING1 mutations in tumors (28–37) only 0.27% of sporadic breast cancers and 3.5% of

brain tumors have an ING1 mutation (28); instead, deregulation and mislocalization of ING1B appears to occur. However, it is possible that we also have underestimated the frequency of mutations in these studies for at least two technical reasons. First, PCR-SSCP analysis is not 100% sensitive for the detection of mutations. Second, and more importantly, these SSCP analyses were carried out over regions spanning ~75% of the currently known ING1 coding region, thereby leaving open the possibility that mutations outside these regions may not have been detected. Determination of the complete genomic structure of the ING1 gene, and analysis of the entire coding region and intron-exon boundaries of alternative splice products are presently being undertaken, and will help to refine our estimate of the mutation rate in brain tumors and other cancers.

Similar to recent observations from studies on ING1 in melanoma cell lines (39), we observed a low frequency of mutations and increased expression of ING1B in primary brain tumors and glioma cell lines compared with normal controls. These data sharply contrast with results derived from studies on squamous cell carcinomas, where significant rates of mutation were reported (31–33), or with other tumors in which ING1B was down-regulated significantly (28–30, 34–37). However, we cannot exclude the possibility that tumor-specific post-translational modifications of $p33^{ING1b}$ may be important in the pathophysiology of human brain tumors. As shown in Fig. 3*A*, highly antigenic proteins other than $p33^{ING1b}$ and $p47^{ING1a}$ cross-reacted with ING1 antibodies, but only in the tumor samples. These proteins may represent unknown ING1 splicing variants or tumor-specific, post-translationally modified or mutated forms of $p33^{ING1b}$. It is possible that these uncharacterized putative ING1 isoforms could have relevant biological functions in the pathophysiology of brain tumors, so that deregulation of ING1B could have an effect on the functions of these proteins (4, 10).

Finally, we have found that $p33^{ING1b}$ displayed cytoplasmic localization in all of the analyzed glioma samples and in some glioma cell lines. This is similar to certain tumors such as melanoma (35, 36), seminoma (35), papillary thyroid carcinoma (35), ductal breast carcinoma (35), and acute lymphoblastic leukemia (35, 37), where $p33^{ING1b}$ was reported to localize predominantly to the cytoplasm, although $p33^{ING1b}$ contains a nuclear localization signal (7). In light of recent reports identifying candidate mutations of $p33^{ING1b}$ in its plant homeo domain and nuclear translocation sequence (31–33), it is possible that the cytoplasmic distribution of $p33^{ING1b}$ we observed could represent undetected mutations in these sequences that could alter function. Indeed, we have demonstrated previously that altered subcellular localization of $p33^{ING1b}$ abrogates its pro-apoptotic functions (7). Alternatively, loss of targeting factors that ensure the proper intracellular localization of $p33^{ING1b}$ or its physical association with p53 could account for the abnormal localization of $p33^{ING1b}$ in brain tumors. These results resemble those reported for p53 in some brain tumors in which p53 has shown to localize to the cytoplasm (52). Recent experimental observations, including post-translational stabilization of p53 by $p33^{ING1b}$ (14) and the discovery of the p53 cytoplasmic-anchoring ubiquitin ligase Parc (53) and its p53-regulatory role (53), support these last possibilities. Alterations in either of these mechanisms would be expected to have profound consequences in the subcellular localization and biological functions of $p33^{ING1b}$.

Our data indicate that genetic alteration of ING1 is not a major factor in the development of brain tumors. However, the expression of ING1B was highly variable in tumor specimens compared with normal brain. This variability could mean that only very large changes of expression would be considered "statistically" significant for the group of tumors as a whole, whereas biologically significant differences in tumor suppressor function may occur in a few individual tumors. Although this and several other recent studies (35–37, 39) support the idea that dysregulation and mislocalization $p33^{ING1b}$ contribute to the generation of specific tumors, additional studies aimed at additionally characterizing the functional interactions between $p33^{ING1b}$ and p53, as well as studying the effects of altering the localization of $p33^{ING1b}$, will make clearer what biological effects may result from mislocalization and deregulated expression of $p33^{ING1b}$.

ACKNOWLEDGMENTS

We thank D. Boland and the Southern Alberta Cancer Research Center Hybridoma Facility for antibody production, Dr. Ramsay of the Canadian Brain Tumor Tissue Bank (London, Ontario, Canada) for supplying some of the brain tumor and normal brain specimens, and Dr. W. Yong and T. Wilson for supplying human fetal astrocyte cultures. We would also like to thank Drs. Gavin Stuart and Tom Feasby for support of this project.

REFERENCES

1. Ma, D., Lawless, D., and Riabowol, K. Correction and addition to ING1 sequences. Nat. Genet., *23:* 373, 1999.

2. Garkavtsev, I., Kazarov, A., Gudkov, A., and Riabowol, K. Suppression of the novel growth inhibitor p33ING1 promotes neoplastic transformation. Nat. Genet., *14:* 415–420, 1996.

3. Garkavtsev, I., Grigorian, I. A., Ossovskaya, V. S., Chernov, M. V., Chumakov, P. M., and Gudkov, A. V. The candidate tumour suppressor p33ING1 cooperates with p53 in cell growth control. Nature (Lond.), *391:* 295–298, 1998.

4. Vieyra, D., Toyama, T., Hara, Y., Boland, D., Johnston, R., and Riabowol, K. ING1 isoforms differentially affect apoptosis in a cell age-dependent manner. Cancer Res., *62:* 4445–4452, 2002.

5. Helbing, C. C., Veillette, C., Riabowol, K., Johnston, R. N., and Garkavtsev, I. A novel candidate tumor suppressor, ING1, is involved in the regulation of apoptosis. Cancer Res., *57:* 1255–1258, 1997.

6. Shinoura, N., Muramatsu, Y., Nishimura, M., Yoshida, Y., Saito, A., and Yokoyama, T., Furukawa, T., Horii, A., Hashimoto, M., Asai, A., Kirino, T., and Hamada, H. Adenovirus-mediated transfer of p33ING1 with p53 drastically augments apoptosis in gliomas. Cancer Res., *59:* 5521–5528, 1999.

7. Scott, M., Boisvert, F. M., Vieyra, D., Johnston, R. N., Bazett-Jones, D. P., and Riabowol, K. UV induces nucleolar translocation of ING1 through two distinct nucleolar targeting sequences. Nucleic Acids Res., *29:* 2052–2058, 2001.

8. Scott, M., Bonnefin, P., Vieyra, D., Boisvert, F. M., Young, D., Bazett-Jones, D. P., and Riabowol, K. UV-induced binding of ING1 to PCNA regulates the induction of apoptosis. J. Cell Sci., *114:* 3455–3462, 2001.

9. Shimada, H., Liu, T. L., Ochiai, T., Shimizu, T., Haupt, Y., Hamada, H., Abe, T., Oka, M., Takiguchi, M., and Hiwasa, T. Facilitation of adenoviral wild-type p53-induced apoptotic cell death by overexpression of p33(ING1) in T. Tn human esophageal carcinoma cells. Oncogene, *21:* 1208–1216, 2002.

10. Vieyra, D., Loewith, R., Scott, M., Bonnefin, P., Boisvert, F. M., Cheema, P., Pastyryeva, S., Meijer, M., Johnston, R. N., Bazett-Jones,

D. P., McMahon, S., Cole, M. D., Young, D., and Riabowol, K. Human ING1 proteins differentially regulate histone acetylation. J. Biol. Chem., *277:* 29832–29839, 2002.

11. Cheung, K. J., Jr., and Li, G. p33(ING1) enhances UVB-induced apoptosis in melanoma cells. Exp. Cell Res., *279:* 291–298, 2002.

12. Nagashima, M., Shiseki, M., Miura, K., Hagiwara, K., Linke, S. P., Pedeux, R., Wang, X. W., Yokota, J., Riabowol, K., and Harris, C. C. DNA damage-inducible gene p33ING2 negatively regulates cell proliferation through acetylation of p53. Proc. Natl. Acad. Sci. USA, *98:* 9671–9676, 2001.

13. Takahashi, M., Seki, N., Ozaki, T., Kato, M., Kuno, T., Nakagawa, T., Watanabe, K., Miyazaki, K., Ohira, M., Hayashi, S., Hosoda, M., Tokita, H., Mizuguchi, H., Hayakawa, T., Todo, S., and Nakagawara, A. Identification of the p33(ING1)-regulated genes that include cyclin B1 and proto-oncogene DEK by using cDNA microarray in a mouse mammary epithelial cell line NMuMG. Cancer Res., *62:* 2203–2209, 2002.

14. Leung, K. M., Po, L. S., Tsang, F. C., Siu, W. Y., Lau, A., Ho, H. T., and Poon, R. Y. The candidate tumor suppressor ING1b can stabilize p53 by disrupting the regulation of p53 by MDM2. Cancer Res., *62:* 4890–4893, 2002.

15. Cheung, K. J., Jr., Mitchell, D., Lin, P., and Li, G. The tumor suppressor candidate p33(ING1) mediates repair of UV-damaged DNA. Cancer Res., *61:* 4974–4977, 2001.

16. Skowyra, D., Zeremski, M., Neznanov, N., Li, M., Choi, Y., Uesugi, M., Hauser, C. A., Gu, W., Gudkov, A. V., and Qin, J. Differential association of products of alternative transcripts of the candidate tumor suppressor ING1 with the mSin3/HDAC1 transcriptional corepressor complex. J. Biol. Chem., *276:* 8734–8739, 2001.

17. Feng, X., Hara, Y., and Riabowol, K. Different HATS of the ING1 gene family. Trends Cell Biol., *12:* 532–538, 2002.

18. Garkavtsev, I., Demetrick, D., and Riabowol, K. Cellular localization and chromosome mapping of a novel candidate tumor suppressor gene (ING1). Cytogenet. Cell Genet., *76(3–4):* 176–178, 1997.

19. Motomura, K., Nishisho, I., Takai, S., Tateishi, H., Okazaki, M., Yamamoto, M., Miki, T., Honjo, T., and Mori. T. Loss of alleles at loci on chromosome 13 in human primary gastric cancers. Genomics, *2:* 180–184, 1988.

20. Rasheed, B. K., and Bigner, S. H. Genetic alterations in glioma and medulloblastoma. Cancer Metastasis Rev., *10:* 289–299, 1991.

21. Yang-Feng, T. L., Li, S., Han, H., and Schwartz, P. E. Frequent loss of heterozygosity on chromosomes Xp and 13q in human ovarian cancer. Int. J. Cancer, *52:* 575–580, 1992.

22. Mostert, M. M., van de Pol, M., Olde Weghuis, D., Suiklerbuijk, R. F., Geurts van Kessel, A., van Echten, J., Oosterhuis, J. W., and Looijenga, L. H. Comparative genomic hybridization of germ cell tumors of the adult testis: confirmation of karyotypic findings and identification of a 12p-amplicon. Cancer Genet. Cytogenet., *89:* 146–152, 1996.

23. Maestro, R., Piccinin, S., Doglioni, C., Gasparotto, D., Vukosavljevic, T., Sulfaro, S., Barzan, L., and Boiocchi, M. Chromosome 13q deletion mapping in head and neck squamous cell carcinomas: identification of two distinct regions of preferential loss. Cancer Res., *56:* 1146–1150, 1996.

24. Leonard, C., and Huret, J. L. From cytogenetics to cytogenomics of bladder cancers. Bull. Cancer., *89:* 166–173, 2002.

25. Weber, R. G., Sabel, M., Reifenberger, J., Sommer, C., Oberstrass, J., Reifenberger, G., Kiessling, M., and Cremer, T. Characterization of genomic alterations associated with glioma progression by comparative genomic hybridization. Oncogene, *13:* 983–994, 1996.

26. Harada, K., Nishizaki, T., Ozaki, S., Kubota, H., Ito, H., and Sasaki, K. Intratumoral cytogenetic heterogeneity detected by comparative genomic hybridization and laser scanning cytometry in human gliomas. Cancer Res., *58:* 4694–4700, 1998.

27. Patel, A., Van Meyel, D. J., Mohapatra, G., Bollen, A., Wrensch, M., Cairncross, J. G., and Feuerstein, B. G. Gliomas in families: chromosomal analysis by comparative genomic hybridization. Cancer Genet. Cytogenet., *100:* 77–83, 1998.

28. Toyama, T., Iwase, H., Watson, P., Muzik, H., Saettler, E., Magliocco, A., DiFrancesco, L., Forsyth, P., Garkavtsev, I., Kobayashi, S., and Riabowol, K. Suppression of ING1 expression in sporadic breast cancer. Oncogene, *18:* 5187–5193, 1999.

29. Ohgi, T., Masaki, T., Nakai, S., Morishita, A., Yukimasa, S., Nagai, M., Miyauchi, Y., Funaki, T., Kurokohchi, K., Watanabe, and S., Kuriyama, S. Expression of p33(ING1) in hepatocellular carcinoma: relationships to tumour differentiation and cyclin E kinase activity. Scand. J. Gastroenterol., *37:* 1440–1448, 2002.

30. Oki, E., Maehara, Y., Tokunaga, E., Kakeji, Y., and Sugimachi, K. Reduced expression of p33(ING1) and the relationship with p53 expression in human gastric cancer. Cancer Lett., *147:* 157–162, 1999.

31. Gunduz, M., Ouchida, M., Fukushima, K., Hanafusa, H., Etani, T., Nishioka, S., Nishizaki, K., and Shimizu, K. Genomic structure of the human ING1 gene and tumor-specific mutations detected in head and neck squamous cell carcinomas. Cancer Res., *60:* 3143–3146, 2000.

32. Chen, L., Matsubara, N., Yoshino, T., Nagasaka, T., Hoshizima, N., Shirakawa, Y., Naomoto, Y., Isozaki, H., Riabowol, K., and Tanaka, N. Genetic alterations of candidate tumor suppressor ING1 in human esophageal squamous cell cancer. Cancer Res., *61:* 4345–4349, 2001.

33. Hoque, M. O., Kawamata, H., Nakashiro, K., Omotehara, F., Hino, S., Uchida, D., Harada, K., Begum, N. M., Yoshida, H., Sato, M., and Fujimori, T. Dysfunction of the p53 tumor suppressor pathway in head and neck cancer. Int. J. Oncol., *21:* 119–126, 2002.

34. Ohmori, M., Nagai, M., Tasaka, T., Koeffler, H. P., Toyama, T., Riabowol, K., and Takahara, J. Decreased expression of p33ING1 mRNA in lymphoid malignancies. Am. J. Hematol., *62:* 118–119, 1999.

35. Nouman, G. S., Angus, B., Lunec, J., Crosier, S., Lodge, A., and Anderson, J. J. Comparative assessment expression of the inhibitor of growth 1 gene (ING1) in normal and neoplastic tissues. Hybrid Hybridomics, *21:* 1–10, 2002.

36. Nouman, G. S., Anderson, J. J., Mathers, M. E., Leonard, N., Crosier, S., Lunec, J., and Angus, B. Nuclear to cytoplasmic compartment shift of the p33ING1b tumour suppressor protein is associated with malignancy in melanocytic lesions. Histopathology, *40:* 360–366, 2002.

37. Nouman, G. S., Anderson, J. J., Wood, K. M., Lunec, J., Hall, A. G., Reid, M. M., and Angus, B. Loss of nuclear expression of the p33(ING1b) inhibitor of growth protein in childhood acute lymphoblastic leukaemia. J. Clin. Pathol., *55:* 596–601, 2002.

38. Sager, R. Expression genetics in cancer: shifting the focus from DNA to RNA. Proc. Natl. Acad. Sci. USA, *94:* 952–955, 1997.

39. Campos, E. I., Cheung, K. J., Jr., Murray, A., Li, S., and Li, G. The novel tumour suppressor gene ING1 is overexpressed in human melanoma cell lines. Br. J. Dermatol., *146:* 574–580, 2002.

40. Zeremski, M., Hill, J. E., Kwek, S. S., Grigorian, I. A., Gurova, K. V., Garkavtsev, I. V., Diatchenko, L., Koonin, E. V., and Gudkov, A. V. Structure and regulation of the mouse ing1 gene. Three alternative transcripts encode two phd finger proteins that have opposite effects on p53 function. J. Biol. Chem., *274:* 32172–32181, 1999.

41. Garkavtsev, I., and Riabowol, K. Extension of the replicative life span of human diploid fibroblasts by inhibition of the p33ING1 candidate tumor suppressor. Mol. Cell. Biol., *17:* 2014–2019, 1997.

42. Pollack, I. F., Finkelstein, S. D., Woods, J., Burnham, J., Holmes, E. J., Hamilton, R. L., Yates, A. J., Boyett, J. M., Finlay, J. L., and Sposto, R. Expression of p53 and prognosis in children with malignant gliomas. N. Engl. J. Med., *346:* 420–427, 2002.

43. Collins, V. P., and James, C. D. Gene and chromosomal alterations associated with the development of human gliomas. FASEB J., *7:* 926–930, 1993.

44. James, C. D., and Collins, V. P. Molecular genetic characterization of CNS tumor oncogenesis. Adv. Cancer Res., *58:* 121–142, 1992.

45. Hollstein, M., Sidransky, D., Vogelstein, B., and Harris, C. C. p53 mutations in human cancers. Science (Wash. DC), *253:* 49–53, 1991.

46. Sambrook, J., Fritsch, E. F., and Maniatis, T. Chapter 10. Preparation of radiolabeled DNA and RNA probes. *In:* Molecular Cloning. A Laboratory Manual. Second Ed., pp. 10.60–10.70. Cold Spring Harbor: Cold Spring Harbor Laboratory Press, 1989.

47. Chomczynski, P., and Sacci, N. Single-step method of RNA isolation by acid guanidinium thiocyanate-phenol-chloroform extraction. Anal. Biochem., *162:* 156–159, 1987.

48. Wong, H., Anderson, W. D., Cheng, T., and Riabowol, K. Monitoring mRNA expression by polymerase chain reaction: the "primer-dropping" method. Anal. Biochem., *223:* 251–258, 1994.

49. Boland, D., Olineck, V., Bonnefin, P., Vieyra, D., Parr, E., and Riabowol, K. A panel of CAb antibodies recognize endogenous and ectopically expressed ING1 protein. Hybridoma, *19:* 161–165, 2000.

50. Riabowol, K. T., Draetta, G., Brizuela, L., Vandre, D., and Beach, D. The cdc2 kinase is a nuclear protein that is essential for mitosis in mammalian cells. Cell, *57:* 393–401, 1989.

51. Yaffe, M. B., Leparc, G. G., Lai, J., Obata, T., Volinia, S., and Cantley, L. C. A motif-based profile scanning approach for genome wide prediction of signaling pathways. Nature Biotech., *19:* 348–353, 2001.

52. Moll, U. M., LaQuaglia, M., Benard, J., and Riou, G. Wild-type p53 protein undergoes cytoplasmic sequestration in undifferentiated neuroblastomas but not in differentiated tumors. Proc. Natl. Acad. Sci. USA, *92:* 4407–4411, 1995.

53. Nikolaev, A. Y., Li, M., Puskas, N., Qin, J., and Gu, W. Parc: a cytoplasmic anchor for p53. Cell, *112:* 29–40, 2003.